

1 **Identification of a novel lineage bat SARS-related coronaviruses that use bat**

2 **ACE2 receptor**

3 Hua Guo^{a,b#}, Ben Hu^{a#}, Hao-rui Si^{a,b#}, Yan Zhu^a, Wei Zhang^a, Bei Li^a, Ang Li^{a,b}, Rong

4 Geng^{a,b}, Hao-Feng Lin^{a,b}, Xing-Lou Yang^a, Peng Zhou^{a*}, Zheng-Li Shi^{a*}

5

6 a. CAS Key Laboratory of Special Pathogens and Biosafety, Wuhan Institute of Virology,

7 Center for Biosafety Mega-Science, Chinese Academy of Sciences, Wuhan 430071, China.

8 b. University of Chinese Academy of Sciences, Beijing, 100049, China.

9

10 #These authors contributed equally.

11 *To whom correspondence should be addressed: peng.zhou@wh.iov.cn;

12 zlshi@wh.iov.cn

13

14 **Author contributions**

15 Z-L.S and P.Z. conceived the study. X-L.Y organized sampling. B.H., H-R.S, B.L.

16 and Y.Z. performed viral genome sequencing and bioinformatics analysis. H.G., W.Z.,

17 A.L. and R.G. performed protein expression and RBD-ACE2 binding assays. H.G.

18 and H-F.L. performed pseudovirus work. H.G, H.B, P.Z and Z-L.S wrote the paper

19 with input from all authors.

20

21

22 **Abstract**

23 Severe respiratory disease coronavirus-2 (SARS-CoV-2) causes the most devastating
24 disease, COVID-19, of the recent century. One of the unsolved scientific questions
25 around SARS-CoV-2 is the animal origin of this virus. Bats and pangolins are
26 recognized as the most probable reservoir hosts that harbor the highly similar SARS-
27 CoV-2 related viruses (SARSr-CoV-2). Here, we report the identification of a novel
28 lineage of SARSr-CoVs, including RaTG15 and seven other viruses, from bats at the
29 same location where we found RaTG13 in 2015. Although RaTG15 and the related
30 viruses share 97.2% amino acid sequence identities to SARS-CoV-2 in the conserved
31 ORF1b region, but only show less than 77.6% to all known SARSr-CoVs in genome
32 level, thus forms a distinct lineage in the *Sarbecovirus* phylogenetic tree. We then
33 found that RaTG15 receptor binding domain (RBD) can bind to and use *Rhinolophus*
34 *affinis* bat ACE2 (RaACE2) but not human ACE2 as entry receptor, although which
35 contains a short deletion and has different key residues responsible for ACE2 binding.
36 In addition, we show that none of the known viruses in bat SARSr-CoV-2 lineage or
37 the novel lineage discovered so far use human ACE2 efficiently compared to SARSr-
38 CoV-2 from pangolin or some of the SARSr-CoV-1 lineage viruses. Collectively, we
39 suggest more systematic and longitudinal work in bats to prevent future spillover
40 events caused by SARSr-CoVs or to better understand the origin of SARS-CoV-2.

41

42

43 **Keywords:** SARS-related coronavirus, Novel lineage, Bat, Reservoir host, ACE2,

44

45

46 **Introduction**

47 SARS-CoV-2, a novel coronavirus that causes COVID-19 which was first identified
48 in late 2019 [1], took just a few months to sweep the globe. As the largest pandemic
49 in the past century in human history, it not only results in serious impact on human
50 health but also leads to stagnation in economics, travel, education and many other
51 societal functions globally.

52

53 The natural origin of SARS-CoV-2 is one of the unanswered scientific questions
54 about the COVID-19 pandemic. It is generally believed that SARS-CoV-2 is
55 transmitted from an animal reservoir host to human society through an or multiple
56 intermediate hosts [2]. The discovery of SARS-CoV-2 related viruses (SARSr-CoV-
57 2), RaTG13 and Pangolin-CoV from horseshoe bats and pangolin respectively, shed
58 light on the importance of these two groups as animal reservoirs of SARSr-CoV-2
59 viruses [1,3,4]. However, among the six critical residues of the receptor-binding
60 domain (RBD) in spike to interact with human ACE2 receptor, RaTG13 only shares
61 one with SARS-CoV-2 [5]. The RBD of RaTG13 has a lower binding affinity and
62 usage efficiency with human ACE2 though sharing 96% genome sequence identity to
63 SARS-CoV-2 [6-8]. One of the viruses derived from Malayan pangolin (*Manis*
64 *javanica*), Pangolin-CoV-GD, possesses six identical critical residues of RBD with
65 SARS-CoV-2 and displays a similar binding affinity to human ACE2 compared with
66 SARS-CoV-2, although it shares lower sequence identity to SARS-CoV-2 in genome
67 compared with RaTG13 [4,7,8]. Another SARSr-CoV-2 detected from bat
68 (*Rhinolophus malayanus*), RmYN02, contains a similar insertion at the S1/S2
69 cleavage site in the spike of SARS-CoV-2, but it has some deletions in the RBD and
70 fails to bind with human ACE2 [9]. Besides, more SARSr-CoV-2 viral genome

71 sequences from bats have been reported from Eastern China, Japan, and Southeast
72 Asian countries subsequently [10-13]. However, the progenitor virus that shares
73 >99% identical to SARS-CoV-2 was still undetermined.

74

75 Bats also carry SARSr-CoV with all the genetic building blocks of SARS-CoV-1,
76 which jumped to human in 2002 [14]. Therefore, investigation of bat SARSr-CoVs is
77 not only important for tracing the origin and immediate progenitor viruses of SARS-
78 CoV-2, but also critical for public health measures to prevent future outbreaks caused
79 by this species of viruses. Here, we report the genome characterization and viral
80 receptor analysis of a novel lineage of SARSr-CoVs in Tongguan town, Mojiang
81 county, Yunnan province in China in 2015, the same location where we found bat
82 RaTG13 in 2013 [1].

83

84 **Methods**

85 ***Bat Sampling and Coronavirus Detection***

86 Sampling of bat was conducted in Mojiang county, Yunnan province at May 2015.
87 Bats were released after anal swabs sampling. Samples were aliquoted and stored at -
88 80 °C until use. RNA was extracted using the High Pure Viral RNA Kit (Roche,
89 Basel, Switzerland). Partial RdRp was amplified using the SuperScript III OneStep
90 RT-PCR and Platinum Taq Enzyme kit (Invitrogen, Carlsbad, CA, USA) by family-
91 specific degenerate seminested PCR. The PCR products were gel purified and
92 sequenced with an ABI Prism 3700 DNA analyzer (Applied Biosystems, Foster City,
93 CA). The sequences were blasted against the GenBank database.

94

95 ***Genome Sequencing***

96 For SARSr-CoV positive RNA extractions, next-generation sequencing (NGS) was
97 performed using BGI MGISEQ 2000. NGS reads were first processed by Cutadapt
98 (v.1.18) to eliminate the possible contamination. Then the clean reads were assembled
99 into genomes using Geneious (v11.0.3) and MEGAHIT (v1.2.9). PCR and Sanger
100 sequencing were used to fill the genome gaps. To amplify the terminal ends, a
101 SMARTer RACE 5`/3`kit (Takara) was used. Bat species identification was based on
102 the partial sequence of cytochrome c oxidase subunit I (COI) gene.

103

104 *Phylogenetic Analysis*

105 Routine sequence management and analysis were carried out using DNASTar.
106 Sequence alignments were created by ClustalW implemented in MEGA6 with default
107 parameters. Maximum Likelihood and Neighbour-joining phylogenetic trees were
108 generated using the Jukes-Cantor model with 1000 bootstrap replicates in the MEGA6
109 software package. Similarity plot analysis of the full-length genome sequences was
110 conducted by Simplot 3.5.1. The genome ID used in the analysis are MN996528 for
111 SARS-CoV-2, AY278488 for SARS-CoV-1, MN996532 for the bat SARSr-CoV
112 RaTG13, MG772933 for ZC45, MW251308 for RacCS203, LC556375 for Rc-o319,
113 KF367457 for WIV1, DQ022305 for HKU3-1, MT121216 for pangolin-CoV-GD
114 strain, MT072864.1 for pangolin-CoV-GX strain, EPI_ISL_412977 for bat SARSr-
115 CoV RmYN02, EPI_ISL_852604 for RshSTT182. The National Genomics Data
116 Center of China ID for the eight novel lineage SARSr-CoVs are:
117 GWHBAUM01000000- GWHBAUT01000000.

118

119 *Expression Constructs, Protein Expression, and Purification*

120 Codon-optimized RBD genes from the following viruses were used (see above
121 genome accession number): SARS-CoV-2 (spike aa 330-583), SARS-CoV-1 (spike aa
122 317–569), RaTG13 (spike aa 330-583), pangolin-CoV-GD (spike aa326-579),
123 pangolin-CoV-GD (spike aa 330-583), RaTG15 (spike aa 317-566). They were
124 synthesized (Sangon Biotech, Shanghai, China) and placed into the expression vector
125 with an N-terminal signal peptide and an S-tag as described previously [15]. The
126 ectodomains of human ACE2 (aa 19–615, accession number: AB046569) and
127 *R.affinis* ACE2 (aa 19–615, accession number: MT394204) were amplified and
128 cloned into the same expression vector as above.

129

130 The RBD and ACE2 proteins used for the BLI binding assay were produced in HEK
131 293T/17 cells. Cells were transiently transfected with expression plasmids using
132 Lipofectamine 3000 (Life Technologies), washed twice with D-Hanks solution 6 h
133 post-transfection, and followed with culturing in fresh 293T FreeStyle expression
134 medium (Life Technologies) at 37°C in a humidified 5% CO₂ incubator. The
135 supernatant were harvested 48 h post-transfection and centrifuged at 4000 × *g* for 10
136 min at 4°C. Clarified supernatant were purified by S-tag agarose beads and eluted
137 with 3 M MgCl₂. The purified protein was finally buffered with PBS and quantified
138 using Qubit 2 Fluorometer (Thermo Fisher Scientific), and stored at -80 °C until use.

139

140 ***Bio-layer Interferometry Binding Assays***

141 Binding assays between RBDs and ACE2 proteins were performed using the Octet
142 RED system (ForteBio, Menlo Park, CA, USA) in 96-well microplates at 30°C with
143 shaking at 1000 rpm as described previously [15]. Briefly, the RBD was biotinylated
144 using EZ-Link NHS-LC-LC-Biotin (Thermo Fisher Scientific, Waltham, MA, USA).

145 The Streptavidin Biosensors were activated for 200s prior to coupling with 50 $\mu\text{g/mL}$
146 biotinylated RBD proteins for 600s. A baseline were collected in the kinetic buffer (1
147 M NaCl, 0.1% BSA, 0.02% Tween-20; pH 6.5) for 200s before immersing the sensors
148 in a 1:2 serial diluted ACE2 proteins for 900s and then dissociation in the same
149 kinetic buffer for another 900s. Data analysis from the ForteBio Octet RED
150 instrument includes reference subtraction. Inter-step correction and Y-alignment were
151 used to minimize tip-dependent variability. Curve fitting were performed in a 1:1
152 model using the Data Analysis Software v7.1 (ForteBio, Menlo Park, CA, USA). The
153 mean K_{on} , K_{off} values were determined with a global fit applied to all data. The
154 coefficient of determination (R^2) for these interactions was close to 1.0.

155

156 ***Pseudovirus Entry Assays***

157 Pseudotyped VSV- ΔG particles were generated as previously described with minor
158 adjustments [16]. Briefly, HEK 293T/17 cells were seeded at 6-well-plate and
159 transfected with plasmids contain codon-optimized SARSr-CoV-2 spike at a 70%
160 confluency using Lipofectamine 3000. At 6 h post-transfection, the medium was
161 replaced with fresh DMEM+10%FBS medium. At 24 h after transfection, cells were
162 incubated with VSV-G-pseudotyped VSV ΔG /Fluc at 37°C for 1 h. Cells were
163 subsequently washed five times and supplied with fresh DMEM + 10% FBS medium
164 + anti-VSV-G antibody (Kerafast). Cell-free supernatants were harvested at 24 h after
165 transduction, then centrifuged at $4000 \times g$ for 10 min at 4°C. The virus particles were
166 used for infection directly.

167

168 The 48-well-plate was treated with Poly-L-lysine solution (Sigma) before seeded
169 HEK293T/17 cells. Cells were transiently transfected with equal amounts of human
170 ACE2, *R. affinis* ACE2 or empty vector plasmids at 70% confluency. At 24 h post-
171 transfection, the cells were incubated with same amounts of S-pseudotyped virions for
172 1 h at 37°C, then washed twice with PBS solution, and supplemented with DMEM
173 containing 10% FBS. Luciferase activity was determined using a GloMax
174 luminometer (Promega Biotech Co. Ltd., Beijing, China) 48 h after infection.
175 Infection experiments were performed independently in triplicate with three technical
176 replications each time.

177

178 ***Quantification of Pseudotyped Virus Particles using RT-PCR***

179 Viral RNA of all VSV-spike pseudovirus particles were extracted from 200ul
180 supernatant using the High Pure Viral RNA Kit (Roche, Cat. No. 11858882001)
181 following the supplier's manual. Quantification of pseudovirus by real-time PCR was
182 performed using HiScript® II One Step qRT-PCR SYBR Green Kit (Vazyme, Cat.
183 No. Q221-01). The gene of VSV P protein were amplified and synthesized *in vitro*
184 using mMESSAGING mMACHINE® Kit (Life technologies, Cat. No. AM1344) to
185 serve as a standard. Viral copy numbers were calculated according to the standard
186 curve. Primers used for transcription *in vitro* were: VSV (P protein)-F1:
187 GTTCGTGAGTATCTCAAGTCCT, VSV (P protein)-R2-T7:
188 TAATACGACTCACTATAGGGAGAGCCTTGATTGTCTTCAATTTCTGG,
189 primers used for real-time PCR were described as previously [17].

190

191 **Results**

192 **Identification of a novel lineage of SARSr-CoVs**

193 In tracing the origin of SARS-CoV-2 from bats, we identified RaTG13, which shares
194 96.2% genome identity to SARS-CoV-2 and is so far the closest genome [1].
195 Following the investigation, we identified eight SARSr-CoV sequences that share
196 93.5% sequence identity to SARS-CoV-2 in the 402-nt partial RdRp gene from bat
197 samples collected at the same place in 2015. Seven samples were from *Rhinolophus*
198 *stheno*, and the other one was from *Rhinolophus affinis* (Table S1). We thus
199 performed next-generation sequencing (NGS) for further analysis of these CoVs.
200 Whole genome sequences were obtained from all eight individual samples. The eight
201 SARSr-CoV genomes are almost identical, sharing more than 99.7% sequence
202 identity among each other. One strain designated RaTG15 was used as the
203 representative in the subsequent analysis.

204

205 In the seven conserved replicase domains used for coronavirus species classification,
206 RaTG15 is 95.3% or 92.5% identical to SARS-CoV-2 and SARS-CoV-1 respectively,
207 suggesting that it remains a member of the *SARSr-CoV* species in the *Sarbecovirus*
208 subgenus within *Betacoronavirus* genus, *Coronaviridae* family. Further, RaTG15 is
209 genetically close to SARS-CoV-2 in open reading frame 1b (ORF1b). In the complete
210 ORF1b region, RaTG15 showed 84.6~89.0% nucleotide identities and 95.6~97.3%
211 amino acid sequence identities to bat SARSr-CoV-2 from wildlife in China and
212 Southeast Asia, which includes bat CoVs RaTG13 and RmYN02 from Yunnan, Rc-
213 o319 from Japan, RshSTT182 from Cambodia, RacCS203 from Thailand, as well as
214 two different strains of pangolin-CoVs (Table S2). It is also conceivable that RaTG15
215 clusters with SARSr-CoV-2 in the phylogeny using full-length RdRp gene (Figure
216 S1A).

217

218 In contrast, similarity plot analysis reveals that beyond ORF1b, RaTG15 is
219 remarkably distinct from both SARSr-CoV-2 and SARSr-CoV-1 in majority of the
220 genome (Figure 1A). It exhibits less than 80% nucleotide identities in ORF1a, M and
221 N genes and lower than 70% identities in S, ORF3, 6 and 7a/7b to all other SARSr-
222 CoVs (Table S2). Overall, the full genome of the SARSr-CoV RaTG15 show 74.4%
223 sequence identity to SARS-CoV-1 and 77.6% to sequence identity to SARS-CoV-2.
224 Notably, RaTG15 show higher sequence identity to SARS-CoV-1 than to SARS-
225 CoV-2 in the spike, E, M, N and ORF6 proteins. It also has almost equivalent
226 homology to any other known SARSr-CoVs from bat or pangolin CoVs (Table S2).
227 This mosaic profile suggests that this novel lineage viruses may be a results of
228 recombination of different SARSr-CoVs.

229

230 The result of phylogenetic analysis is in accordance with similarity plot. SARSr-CoVs
231 mainly consists of two sub-lineages, the SARSr-CoV-1 and SARSr-CoV-2 (Figure
232 1B). The latter one includes SARS-CoV-2 from pangolins and different *Rhinolophus*
233 bats species recently reported in a wide range of areas in Asia. In the full-length
234 genome tree and S gene tree, RaTG15 and the related viruses are distant from both of
235 the two existing sub-lineages, and forms a well-supported novel lineage with the
236 *sarbecoviruses* (Figure 1B and Figure S1B).

237

238 **In silico analysis of receptor binding domain (RBDs) of SARSr-CoVs**

239 We further examined the spike protein sequence of RaTG15 in comparison with other
240 SARSr-CoV-2. The receptor-binding domain (RBD) of the RaTG15 spike is highly
241 divergent from other *sarbecoviruses*, with 72.6% amino acid sequence identity to
242 SARS-CoV-2 and 68.6%-73.3% identities to related bat and pangolin CoVs. Unlike

243 RmYN02 and RacCS203, the RaTG15 RBD does not contain the deletion
244 corresponding to aa 473-486 (deletion 2) of the SARS-CoV-2 spike which determines
245 ACE2 usage based on previous reports [18]. However, aligned with SARS-CoV-2 and
246 RaTG13, a short deletion is noted at the position corresponding to aa 444-447
247 (deletion 1). The location of this deletion is similar to the one in the spike of
248 RshSTT182, a SARS-CoV-2-related CoV identified in *Rhinolophus shameli* from
249 Cambodia. Within the receptor binding motif (RBM), four of the five amino acid
250 residues critical for binding of SARS-CoV-2 to the ACE2 receptor (486, 493, 494 and
251 501) are varied in RaTG15. Like most bat SARSr-CoVs, the polybasic (furin)
252 cleavage site is absent at the S1-S2 junction of RaTG15 (Figure 2).

253

254 **Functional comparison of RBD from three lineages of SARSr-CoVs**

255 The sequence analysis indicated that the RaTG15 virus possibly uses ACE2 as an
256 entry receptor, which was then experimentally confirmed by RBD-ACE2 binding
257 studies using purified recombinant proteins. RBD proteins from SARS-CoV-2,
258 SARS-CoV-1, RaTG13, pangolin-CoV-GD, pangolin-CoV-GX and RaTG15, as well
259 as ectodomains of human and *R.affinis* ACE2 proteins were used (Figure S2A). We
260 found that *R.affinis* derived RaTG13 and RaTG15 RBD proteins either show very
261 weak or have no binding affinity to human ACE2 (HuACE2). In contrast, RBD
262 proteins from the two pangolin SARSr-CoVs displayed much higher binding affinity
263 to HuACE2, only slightly weaker than SARS-CoV-2 RBD but still higher than
264 SARS-CoV-1 (Figure 3A-F and M). Furthermore, the binding affinity to HuACE2 of
265 pangolin-CoV-GX is slightly weaker than pangolin-CoV-GD. Next, we wanted to
266 find out whether bat CoVs RaTG13 and RaTG15 can use *R.affinis* ACE2 more
267 efficiently than huACE2. Detectable binding was observed between RaTG15 RBD

268 and *R.affinis* ACE2 (RaACE2), though the affinity was still weaker than SARS-CoV-
269 2 and pangolin-CoV-GD/GX to RaACE2. RaTG13 RBD showed a very weak binding
270 to RaACE2, same as to HuACE2 (Figure 3G-M and Figure S2B).

271

272 To exclude the possibility that the ACE2 binding of RBD may not represent the
273 functionality of the full-length S protein, we also constructed a VSV-based
274 pseudovirus using previously published method [16]. We produced a list of SARSr-
275 CoVs pseudoviruses, or MERS-CoV pseudovirus as a negative control. HEK293T/17
276 cells overexpression HuACE2, RaACE2 or empty vector were infected with VSV-
277 based pseudoviruses, and the infection efficiency were determined 48 h after
278 infection. Consistent with the RBD-ACE2 protein binding assays, HuACE2 mediated
279 entry of all SARSr-CoVs except the RaTG15, whereas the *R.affinis* ACE2 supported
280 all SARSr-CoVs entry. Notably, RaTG13 pseudovirus infection of HuACE2 or
281 RaACE2-expression cells was minimal, if it is positive, compared to other groups. As
282 control, MERS-CoV pseudovirus failed to infect ACE2-expression cells, confirming
283 ACE2-independent infectivity of VSV backbone (Figure S3). Collectively, none of
284 the SARSr-CoV-2 lineage or the novel lineage virus from bats could efficiently bind
285 to HuACE2 [10,11], and it appears that whether there is deletion at RBD region
286 greatly affecting the binding capacity (Figure 3N). These results suggest that without
287 further adaptation, there is a limited zoonotic potential for bat-derived RaTG13,
288 RaTG15 and perhaps other SARSr-CoV-2 lineage or the novel lineage viruses. In
289 contrast, there is a high spillover potential of pangolin-CoV in the context of cell
290 receptor usage.

291

292 **Discussion**

293 Overall, we report the discovery of a novel lineage of SARSr-CoVs from bats that are
294 closely related to SARS-CoV-2 in the RdRp region, but genetically distant to any
295 known SARSr-CoVs at genome level. Although several SARS-CoV-2 related
296 coronaviruses have been detected from wildlife, none of them shared >99%
297 genetically identical to SARS-CoV-2 at the genome level. Recombination events
298 happen commonly in coronaviruses and can be referred to as potential origin of the
299 progenitor of SARS-CoV-1, as SARSr-CoVs discovered in a bat colony carried all the
300 genomic fragments of SARS-CoV-1 [14,19]. The high sequence similarity to SARS-
301 CoV-2 in some genomic regions detected from different wildlife species implies the
302 recombination may happen during the virus evolution in cross-species or inter-species
303 transmission. The new lineage virus we reported in this study showed weak binding
304 affinity to bat but not human ACE2 though possess one deletion in the RBD of the
305 spike which is different from the previously reported SARSr-CoVs in bat (Figure 2).
306 These results suggested the SARSr-CoVs we discovered from bat now may be just the
307 tip of the iceberg. These viruses may have experienced selection or recombination
308 events in the animal hosts and render viral adaption to a new host then spread to the
309 new species before they jumped into human society. So surveillance to this new
310 lineage virus should be conducted to prevent future outbreaks, as viruses from the
311 other two lineages of SARSr-CoV caused SARS and COVID-19, respectively [1,20].
312 Furthermore, none of the bat SARSr-CoV-2 lineage or the novel lineage viruses
313 discovered so far could be isolated, or be capable of efficiently using human ACE2,
314 thus pose little spillover potential to human without future adaptation [21]. In
315 comparison, the ACE2 usage virus in bat SARSr-CoV-1 related lineage appears to be
316 more dangerous in the context of cross-species transmission, which has been
317 demonstrated in animal studies [22,23].

318

319 The closest bat CoV to SARS-CoV-2 at this stage, RaTG13 only showed very weak
320 binding affinity to HuACE2. Albeit there is a speculation claiming the possible
321 leaking of RaTG13 from lab that caused SARS-CoV-2, the experiment evidence
322 cannot support it. In contrast, the pangolin-CoV shows strong binding capacity to
323 human or bat ACE2, posing high cross-species potential to human or other species. In
324 the context of SARS-CoV-2 animal origin, there could either be a bat SARSr-CoV
325 closer than RaTG13 that is capable of using HuACE2, or be a pangolin-CoV that
326 obtained higher genome similarity other than spike gene. In future, more systematic
327 and longitudinal sampling of bats, pangolins or other possible intermediate animals is
328 required to better understand the origin of SARS-CoV-2.

329

330 **Acknowledgements**

331 We thank Yun-Zhi Zhang, Ji-Hua Zhou from Yunnan CDC for helping with bat
332 sampling. We also would like to thank Dr. Ding Gao in the WIV Core Facility and
333 Technical Support for his help in Octet RED technology. The work was jointly
334 supported by the Strategic Priority Research Program of the Chinese Academy of
335 Sciences (XDB29010101, to Z-L.S) and China National Science Foundation for
336 Excellent Scholars (81290341 to Z-LS, 81822028 to P.Z.).

337

338 **Declaration of Interests**

339 The authors declare no competing interests.

340

341 **References**

- 342 1. Zhou P, Yang X-L, Wang X-G, et al. A pneumonia outbreak associated with
343 a new coronavirus of probable bat origin. *Nature*. 2020
344 2020/03/01;579(7798):270-273.
- 345 2. Zhou P, Shi ZL. SARS-CoV-2 spillover events. *Science*. 2021 Jan
346 8;371(6525):120-122.
- 347 3. Xiao K, Zhai J, Feng Y, et al. Isolation of SARS-CoV-2-related coronavirus
348 from Malayan pangolins. *Nature*. 2020 2020/07/01;583(7815):286-289.
- 349 4. Lam TT-Y, Jia N, Zhang Y-W, et al. Identifying SARS-CoV-2-related
350 coronaviruses in Malayan pangolins. *Nature*. 2020
351 2020/07/01;583(7815):282-285.
- 352 5. Hu B, Guo H, Zhou P, et al. Characteristics of SARS-CoV-2 and COVID-19.
353 *Nature Reviews Microbiology*. 2021 2021/03/01;19(3):141-154.
- 354 6. Shang J, Ye G, Shi K, et al. Structural basis of receptor recognition by SARS-
355 CoV-2. *Nature*. 2020 2020/05/01;581(7807):221-224.
- 356 7. Wrobel AG, Benton DJ, Xu P, et al. Structure and binding properties of
357 Pangolin-CoV spike glycoprotein inform the evolution of SARS-CoV-2.
358 *Nature communications*. 2021 2021/02/05;12(1):837.
- 359 8. Starr TN, Greaney AJ, Hilton SK, et al. Deep Mutational Scanning of SARS-
360 CoV-2 Receptor Binding Domain Reveals Constraints on Folding and ACE2
361 Binding. *Cell*. 2020 Sep 3;182(5):1295-1310 e20.
- 362 9. Zhou H, Chen X, Hu T, et al. A Novel Bat Coronavirus Closely Related to
363 SARS-CoV-2 Contains Natural Insertions at the S1/S2 Cleavage Site of the
364 Spike Protein. *Curr Biol*. 2020;30(11):2196-2203.e3.
- 365 10. Murakami S, Kitamura T, Suzuki J, et al. Detection and Characterization of
366 Bat Sarbecovirus Phylogenetically Related to SARS-CoV-2, Japan.
367 *Emerging Infectious Disease journal*. 2020;26(12):3025.
- 368 11. Wacharapluesadee S, Tan CW, Maneeorn P, et al. Evidence for SARS-CoV-2
369 related coronaviruses circulating in bats and pangolins in Southeast Asia.
370 *Nature communications*. 2021 2021/02/09;12(1):972.
- 371 12. Hu D, Zhu C, Ai L, et al. Genomic characterization and infectivity of a novel
372 SARS-like coronavirus in Chinese bats. *Emerg Microbes Infect*. 2018 Sep
373 12;7(1):154.
- 374 13. Hul V, Delaune D, Karlsson EA, et al. A novel SARS-CoV-2 related
375 coronavirus in bats from Cambodia. *bioRxiv*. 2021:2021.01.26.428212.
- 376 14. Hu B, Zeng LP, Yang XL, et al. Discovery of a rich gene pool of bat SARS-
377 related coronaviruses provides new insights into the origin of SARS
378 coronavirus. *Plos Pathog*. 2017 Nov;13(11):e1006698.
- 379 15. Guo H, Hu B-J, Yang X-L, et al. Evolutionary Arms Race between Virus and
380 Host Drives Genetic Diversity in Bat Severe Acute Respiratory Syndrome-
381 Related Coronavirus Spike Genes. *J Virol*. 2020;94(20):e00902-20.
- 382 16. Johnson MC, Lyddon TD, Suarez R, et al. Optimized Pseudotyping
383 Conditions for the SARS-COV-2 Spike Glycoprotein. *J Virol*.
384 2020;94(21):e01062-20.
- 385 17. Li Q, Wu J, Nie J, et al. The Impact of Mutations in SARS-CoV-2 Spike on
386 Viral Infectivity and Antigenicity. *Cell*. 2020 Sep 3;182(5):1284-1294 e9.
- 387 18. Ren W, Qu X, Li W, et al. Difference in receptor usage between severe
388 acute respiratory syndrome (SARS) coronavirus and SARS-like
389 coronavirus of bat origin. *J Virol*. 2008 Feb;82(4):1899-907.

- 390 19. Cui J, Li F, Shi ZL. Origin and evolution of pathogenic coronaviruses.
391 Nature reviews Microbiology. 2019 Mar;17(3):181-192.
392 20. Drosten C, Gunther S, Preiser W, et al. Identification of a novel
393 coronavirus in patients with severe acute respiratory syndrome. N Engl J
394 Med. 2003 May 15;348(20):1967-76.
395 21. Yang XL, Hu B, Wang B, et al. Isolation and Characterization of a Novel Bat
396 Coronavirus Closely Related to the Direct Progenitor of Severe Acute
397 Respiratory Syndrome Coronavirus. J Virol. 2015 Dec 30;90(6):3253-6.
398 22. Menachery VD, Yount BL, Jr., Debbink K, et al. A SARS-like cluster of
399 circulating bat coronaviruses shows potential for human emergence. Nat
400 Med. 2015 Dec;21(12):1508-13.
401 23. Menachery VD, Yount BL, Jr., Sims AC, et al. SARS-like WIV1-CoV poised
402 for human emergence. Proc Natl Acad Sci U S A. 2016 Mar
403 15;113(11):3048-53.
404

405

406 **Figure legends**

407 **Figure 1. Discovery of a novel lineage of bat SARSr-CoVs.** (A) Similarity plot
408 analysis based on the full-length genome sequence of bat SARSr-CoV RaTG15. Full-
409 length genome sequences of SARS-CoV-1, SARS-CoV-2, bat and pangolin CoVs
410 related to SARS-CoV-2 were used as reference sequences. The analysis was
411 performed with the Kimura model, a window size of 1500 base pairs and a step size
412 of 150 base pairs. (B) Phylogenetic tree based on complete genome sequences of
413 betacoronaviruses. The trees were constructed by the Neighbour-joining method using
414 the Jukes-Cantor model with bootstrap values determined by 1000 replicates.
415 Bootstraps > 50% are shown. The scale bars represent 0.1 substitutions per nucleotide
416 position. The novel SARSr-CoVs characterized in this study are shown in bold. Ra,
417 *Rhinolophus affinis*; Rst, *Rhinolophus stheno*; Rsh, *Rhinolophus shameli*; Rs,
418 *Rhinolophus sinicus*; Rac, *Rhinolophus acuminatus*; Rm, *Rhinolophus malayanus*; Rc,
419 *Rhinolophus cornutus*; MHV, murine hepatitis virus.

420

421 **Figure 2. Comparison of receptor-binding domain (RBDs) of SARSr-CoVs.** The
422 RBM is shown in pink and the five key residues that contact ACE2 directly are
423 highlighted in green. Comparison of the five critical residues of these SARSr-CoVs
424 are listed in the table. Two deletions in the RBM, aa 444-447 (deletion 1) and aa 473-
425 486 (deletion 2) are indicated by red boxes. GenBank or GISAID entries for each
426 virus can be found in Methods.

427

428 **Figure 3. Binding affinity of SARSr-CoV RBDs to ACE2 from human and**
429 ***R.affinis* bat.** (A-F) Binding of different RBD proteins to human ACE2. (G-L)
430 Binding of different RBD proteins to *R.affinis* ACE2. (M) Comparison of dissociation
431 constants (KD) between different RBD to human and *R.affinis* ACE2. Relative
432 binding is analyzed by comparing with SARS-CoV-2 RBD to human ACE2. (N)
433 Summary of the binding efficiency of different RBD to human or bat ACE2. Y, yes;
434 ND, not determined. Evidences for WIV16-CoV, Rc-o0319, RmYN02 and RacCS213
435 were from previous reports [10,11,21]. The presence of deletion in RBM (related to
436 Figure 2) is indicated. Binding assay of human or *R.affinis* ACE2 to different RBD
437 proteins was measured by Bio-layer interferometry. The parameters of KD value (M),
438 K_{on} (1/M.s), K_{off} (1/s) are shown on the upper right side of the picture. Different
439 RBD proteins were immobilized on the sensors and tested for affinity with graded
440 concentrations of human or *R.affinis* ACE2s. The Y-axis shows the real-time binding
441 response. Values reported representing the global fit to all data. The coefficient of
442 determination (R^2) for these interactions was close to 1.0 (Figure S2B).

443

444 **Figure S1. Phylogenetic tree base on the complete S gene sequences (A) or**
445 **complete RdRp gene sequences (B) of betacoronaviruses.** The trees were

446 constructed by the Maximum-likelihood method using the Jukes-Cantor model with
447 bootstrap values determined by 1000 replicates. Bootstraps > 50% are shown. The
448 scale bars represent 0.1 and 0.05 substitutions per nucleotide position, respectively.
449 The novel SARSr-CoVs characterized in this study are shown in bold. Ra,
450 *Rhinolophus affinis*; Rst, *Rhinolophus stheno*; Rsh, *Rhinolophus shameli*; Rs,
451 *Rhinolophus sinicus*; Rac, *Rhinolophus acuminatus*; Rm, *Rhinolophus malayanus*; Rc,
452 *Rhinolophus cornutus*; MHV, murine hepatitis virus.

453

454 **Figure S2. Binding affinity of SARSr-CoVs RBD proteins to ACE2 from human**

455 **and *R.affinis*.** (A) The purity of different CoV-RBD and ACE2 proteins used for
456 binding assay were analyzed by SDS-PAGE. (B) Binding assay of human or *R.affinis*

457 ACE2 to different RBD proteins measured by Bio-layer interferometry, Related to

458 **Figure 3.** The Y-axis shows the real-time binding response. Values reported

459 representing the global fit to all data. The coefficient of determination (R^2) for these

460 interactions was shown on the upper right.

461

462 **Figure S3. Infectivity analysis of SARSr-CoV spike VSV-pseudoviruses in**

463 **human and *R.affinis* ACE2 expression cells.** HEK293T/17 cells expression

464 human/*R.affinis* ACE2 were infected with SARS-CoV-2 and SARSr-CoV spike-

465 pseudotyped viruses. The infected cell lysis was analyzed by measuring luciferase

466 activities. All results were performed in triplicate from three independent

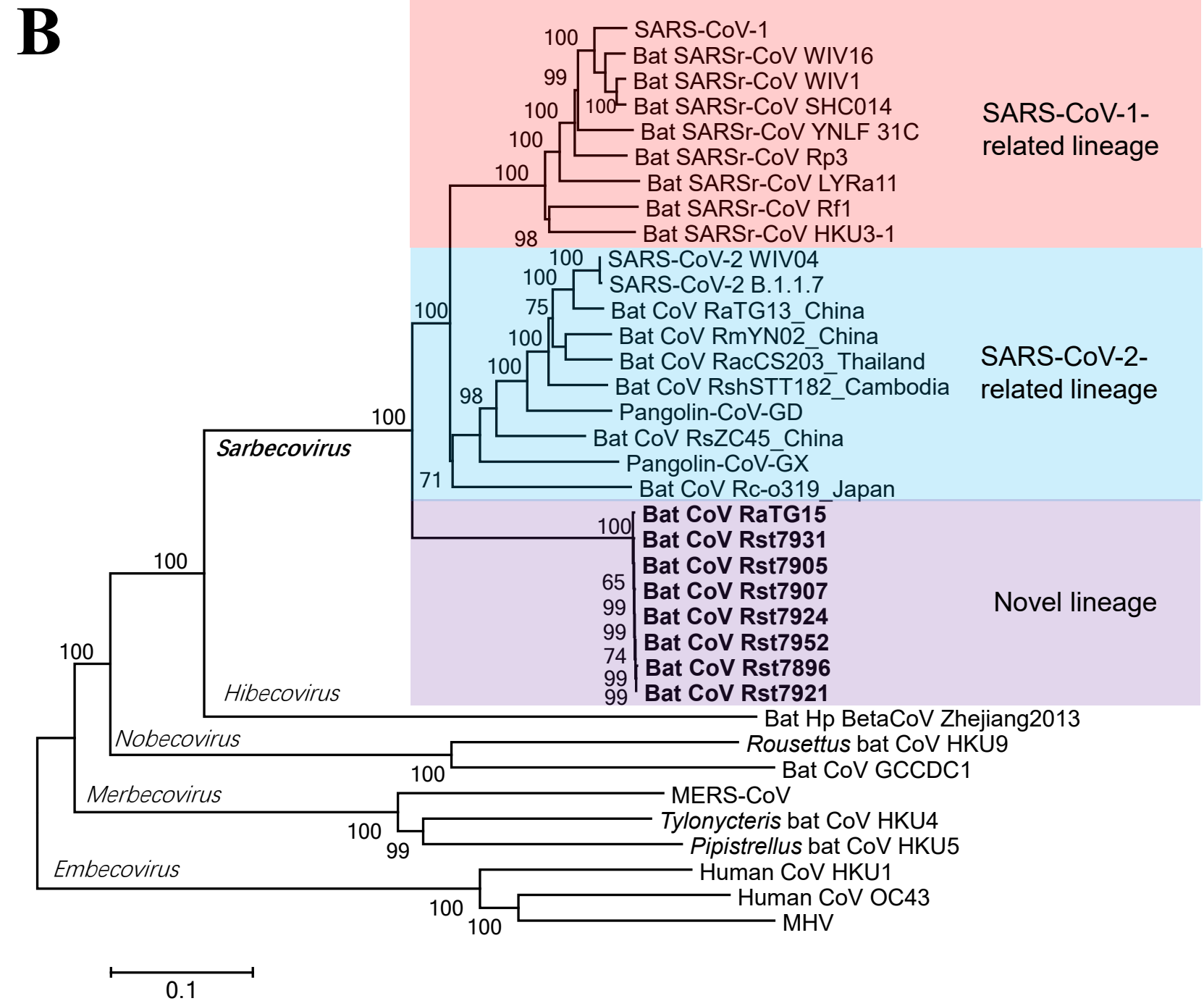
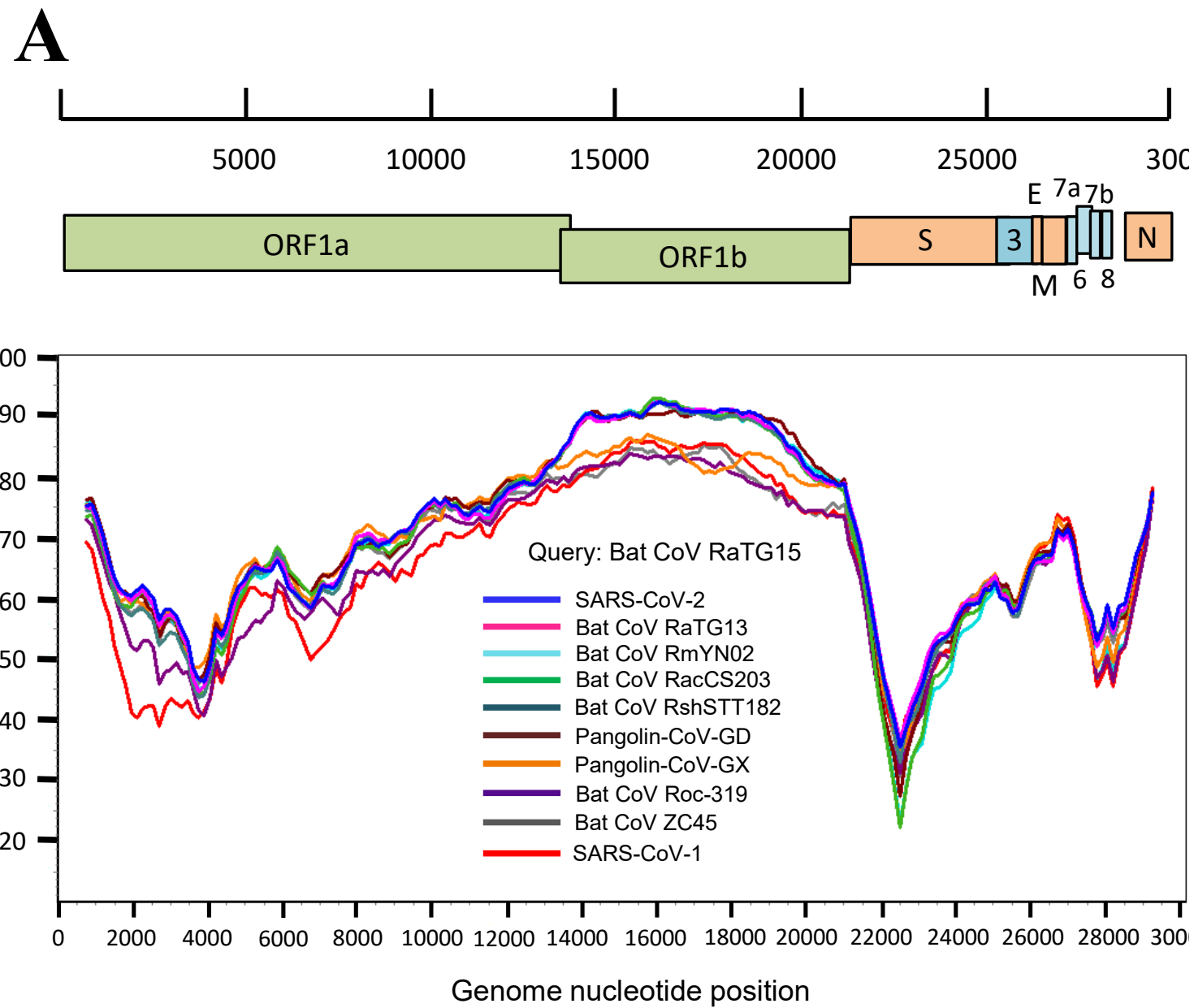
467 experiments. Error bars indicate mean \pm SEM. Statistical significance was tested by

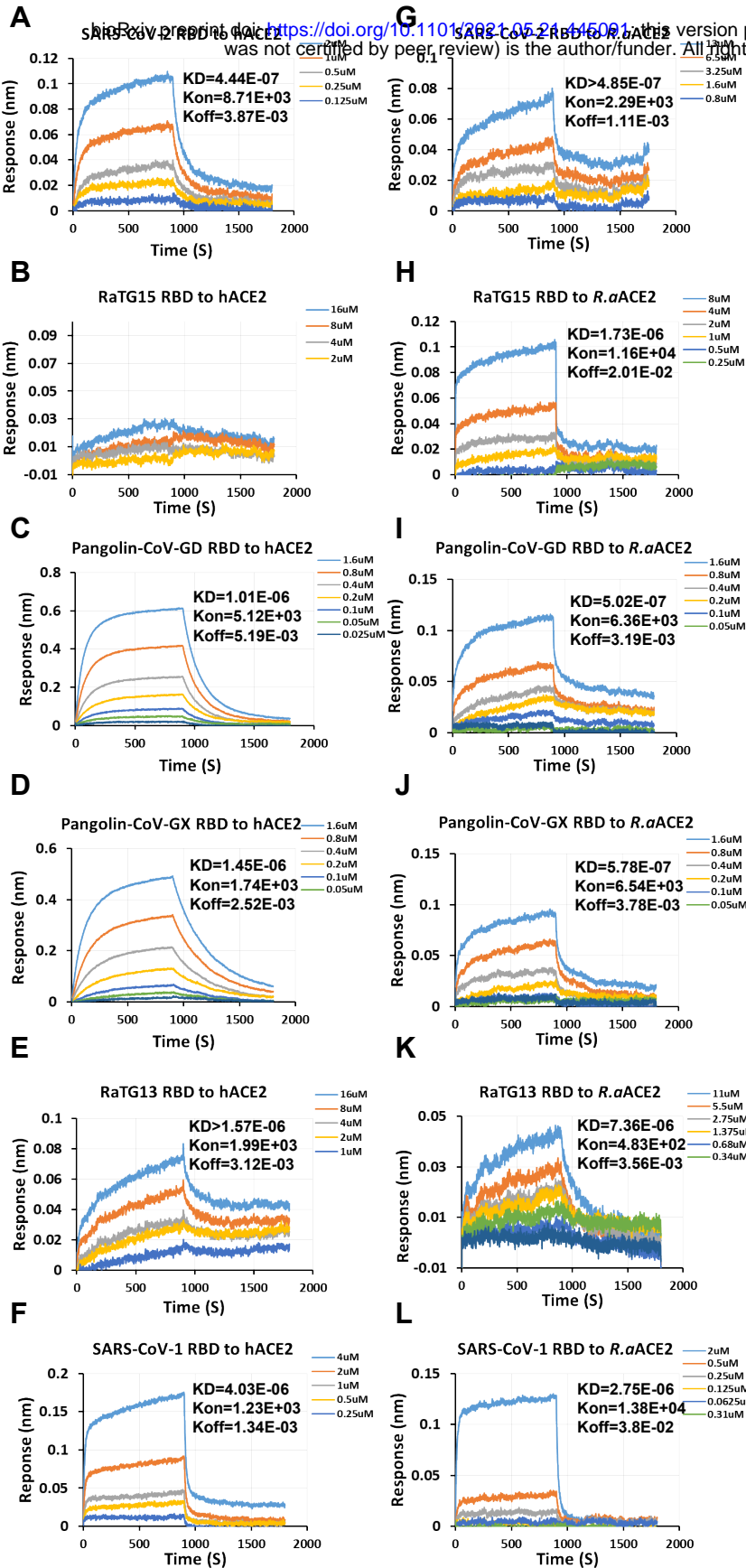
468 one-way ANOVA with Dunnett posttest. (A) SARS-CoV-2, (B) RaTG15, (C)

469 pangolin-CoV-GD, (D) pangolin-CoV-GD, (E) RaTG13, (F) SARS-CoV-1, (G)

470 MERS-CoV. (H) Genome copies of VSV-CoV-S pseudotyped particles. Viral copy

471 numbers were calculated according to the standard curve of VSV P protein gene. A
472 representative result is shown. (I) ACE2 expression was detected using mouse anti-S-
473 tag monoclonal antibody followed by HRP-labelled goat anti-mouse IgG antibody. β -
474 actin was detected with mouse anti- β -action monoclonal antibody by HRP-labelled
475 goat anti-mouse IgG antibody.
476





M SARS-CoV-2 RBD to hACE2. This version posted May 21, 2021. The copyright holder for this preprint (which was not certified by peer review) is the author/funder. All rights reserved. No reuse allowed without permission.

	ACE2	Human	<i>R. affinis</i>
	RBD		
SARS-CoV-2		1.00	>1.09
RaTG15		Not detectable	3.90
Pangolin-CoV-GD		2.28	1.13
Pangolin-CoV-GX		3.26	1.30
RaTG13		Low affinity, >3.53	16.57
SARS-CoV-1		9.07	6.19

N

		Human ACE2	Bat ACE2	Deletion 1	Deletion 2
SARS-CoV-1 related lineage	SARS-CoV-1	✓	✓		
	WIV16-CoV	✓	✓		
	Rp3-CoV	×	×	Y	Y
SARS-CoV-2 related lineage	SARS-CoV-2	✓	✓		
	RaTG13	weak	weak		
	Rc-o0319	×	✓		Y, partial
	RmYN02	×	ND	Y	Y
	RacCS213	×	ND	Y	Y
Novel lineage	Pangolin-CoV-GX	✓	✓		
	Pangolin-CoV-GD	✓	✓		
Novel lineage	RaTG15	×	✓	Y	